

Surface texture generation during cylindrical milling in the aspect of cutting force variations

S Wojciechowski¹, P Twardowski, M Pelic

Poznan University of Technology, Faculty of Mechanical Engineering,
Piotrowo 3, 60-965 Poznan, Poland,

E-mail: sjwojciechowski@o2.pl

Abstract. The work presented here concentrates on surface texture analysis, after cylindrical milling of hardened steel. Cutting force variations occurring in the machining process have direct influence on the cutter displacements and thus on the generated surface texture. Therefore, in these experiments, the influence of active number of teeth (z_c) on the cutting force variations was investigated. Cutting forces and cutter displacements were measured during machining process (online) using, namely piezoelectric force dynamometer and 3D laser vibrometer. Surface roughness parameters were measured using stylus surface profiler. The surface roughness model including cutting parameters (f_z , D) and cutting force variations was also developed. The research revealed that in cylindrical milling process, cutting force variations have immediate influence on surface texture generation.

1. Introduction

The following work is an extension of the previous research [1], related to the surface roughness modelling after finish milling of hardened 55NiCrMoV6 steel. Milling of hardened steels is very often applied to production of drop forging dies and casting moulds [2], because it enables the reduction of technological process through the elimination of some machining operations conducted in a tempered state [3]. Nevertheless, the primary objective of the finish milling process is related to high surface texture quality, which is dependent on the appropriate selection of cutting conditions and tool's geometry.

Previous researches related to the hardened steels milling [4, 5] reveal that basic kinematical – geometrical model is insufficient to the accurate surface roughness estimation. The differences between the measured and calculated surface roughness height values are from 15 to 40 times. These discrepancies are resulting from many various phenomena e.g. plastic and elastic deformations of work material, cutting edge notch, variation of the temperature in the cutting zone, some random factors [6]. However during finish cylindrical milling they are mainly affected by the tool vibrations related to cutter's run out. The majority of works related to surface roughness modelling in milling focus only on static value of cutter's run out [7, 8], which results only from the offset between the position of the tool rotation axis and the spindle rotation axis. Nevertheless, during the machining process, cutter's run out is also affected by some dynamical phenomena related to the instantaneous cutting force values. These cutting forces induce cutter's deflections. Thus, dynamical run out instead of static one

¹ Corresponding author.



affects machined surface roughness. In order to measure cutter's vibrations, during the milling process (online), one can apply laser vibrometer [9] or capacitive gap sensor [10].

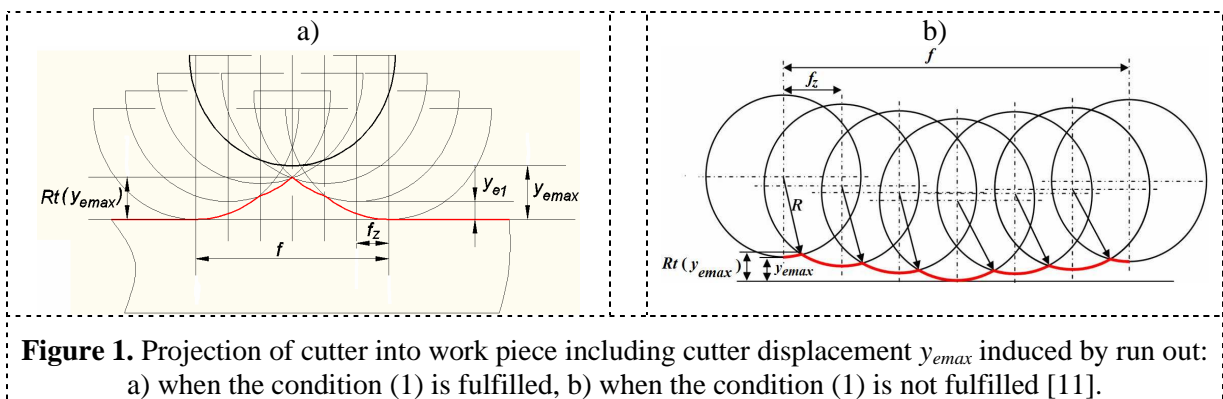
The surface roughness model including cutter displacements developed by the authors of this paper significantly increases the accuracy of the surface roughness parameters estimation, in comparison to theoretic basic model [11]. However this model was only validated in the range of variable feed per tooth values. In this paper, developed model is applied to the surface roughness parameters estimation in the range of variable cutting depth (a_p , a_e), and consequently active number of teeth values. The active number of teeth influences cutting force variations and thus cutter's displacements which have direct effect on the generated surface texture. The calculated cutter's displacements and surface roughness parameters values are compared to those measured by 3D laser vibrometer and stylus surface profiler.

2. Surface roughness model including cutter's displacements in cylindrical milling

Figure 1 depicts surface roughness models including cutter's displacements. The model depicted in Figure 1 is related to the case when the tool rotates around the spindle axis with an eccentricity and the maximum cutter's displacement $y_{e\max}$ per one tool revolution, related to the run out is significantly lower than the tool radius R , $y_{e\max} \ll R$, as well as the radial depth of cut a_e , $y_{e\max} \ll a_e$. For simplification it was assumed that teeth location errors were neglected, which means that partial displacements for consecutive teeth are uniform. It is necessary to emphasize that this assumption can be valid only for monolithic tools. In the case of inserted tools, the influence of insert setting error must be included. From the Figure 1 it is resulting, that in the cylindrical milling process, two different mechanisms of surface irregularities generation can occur. Their appearance (in case when number of teeth $z = 6$) depends on the following condition:

$$f_z < \frac{\sqrt{y_{e\max}(3R - y_{e\max})}}{3} \quad (1)$$

where: R – tool radius.



When the condition (1) is fulfilled (i.e. for small values of feed per tooth and/or large values of cutter's displacement) then surface irregularities are generated by the mechanism presented in figure 1a. In this mechanism surface irregularities formed during cutting process are removed by subsequent positions of teeth, and finally theoretic surface roughness height is lower than cutter's displacement $y_{e\max}$, which from the point of view of surface texture is highly eligible. According to figure 1a, surface roughness height for the $z = 6$ can be calculated from the following equation:

$$Rt(y_{e\max}) = \frac{y_{e\max}}{3} + R - \sqrt{R^2 - 4f_z^2} \quad (2)$$

When the condition (1) is not fulfilled (i.e. for larger values of feed per tooth and/or smaller values of cutter's displacement) then surface irregularities are generated by the mechanism presented in

figure 1b. In this mechanism surface irregularities are at least equal to cutter's displacement $y_{e_{max}}$. According to figure 1a, surface roughness height can be calculated from the following equation:

$$Rt(y_{e_{max}}) = \frac{2(4y_{e_{max}}^2 + f_z^2 \cdot z^2) \cdot (y_{e_{max}} \cdot z) - f_z \cdot z \cdot \sqrt{4y_{e_{max}}^2 + f_z^2 \cdot z^2} \cdot \sqrt{z^2(4R^2 - f_z^2) - 4y_{e_{max}}^2}}{2z \cdot (4y_{e_{max}}^2 + f_z^2 \cdot z^2)} - \frac{2(4y_{e_{max}}^3 - 4R \cdot y_{e_{max}}^2 \cdot z + f_z^2 \cdot y_{e_{max}} \cdot z^2 - f_z^2 \cdot R \cdot z^3)}{2z \cdot (4y_{e_{max}}^2 + f_z^2 \cdot z^2)}, \quad (3)$$

The value of cutter's displacement $y_{e_{max}}$ is resulting both, from cutter's static run out and dynamical phenomena occurring in machining process. Cutter's static run out e_r can be due to tool itself (wear, asymmetry, insert setting, dynamic imbalance and thermal deformation) but it is mainly due to the offset between the position of the tool rotation axis and the spindle rotation axis. The consequence is a tool rotation around the spindle axis with an eccentricity, which induces cutter displacements. Apart from the static run out, cutter's displacement is also affected by some dynamical phenomena related to the cutting and centrifugal force interactions. During the machining process, cutting tool is deflected by cutting forces. This deflection affects the dynamical cutter's run out (which directly affects maximal cutter's displacement per one tool revolution $y_{e_{max}}$). Moreover, at higher rotational speeds $y_{e_{max}}$ value can be also affected by centrifugal forces.

In order to determine cutter's instantaneous displacements $y(t)$ related to cutter's static run and deflections induced by forces one should solve the following equation:

$$y(t) = e_r \cdot \cos\left(\frac{\pi \cdot n \cdot t}{30}\right) - y_d(t) \quad (4)$$

In equation (4) $y_d(t)$ denotes cutter's deflections induced by cutting forces, which can be solved on the basis of differential motion equation:

$$m \cdot \ddot{y}_d(t) + c \cdot \dot{y}_d(t) + k \cdot y_d(t) = F_{fNe}(t) \quad (5)$$

The method of instantaneous feed normal force $F_{fNe}(t)$ determination is discussed in details in the previous work [11]. The example of cutter's instantaneous displacement $y(t)$ chart obtained on the basis of equation (4) is presented in Figure 2. Displacement model parameters were selected from [11]. From figure 2b it can be seen, that during milling with static run out $e_r > 0$ alterations of instantaneous maximal displacements produce the envelope, which has a period equal to tool revolution time T . The height of this envelope is equal to cutter's displacement $y_{e_{max}}$. In case, when static run out $e_r = 0$, no envelope is found and instantaneous maximal displacements per each tooth are uniform (Figure 2a).

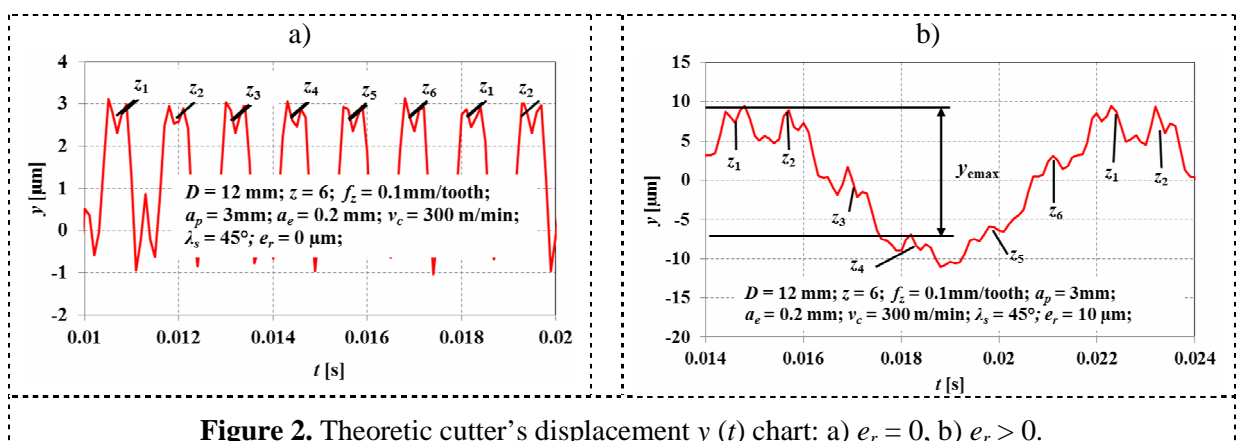


Figure 2. Theoretic cutter's displacement $y(t)$ chart: a) $e_r = 0$, b) $e_r > 0$.

3. Research range and method

The investigations have been carried out on hardened hot-work tool steel plate (55NiCrMoV6, hardness approx. 55 HRC). The monolithic torus mill ($z = 6$ number of teeth, $D = 12$ mm diameter, $r_c = 1$ mm corner radius, $\lambda_s = 45^\circ$ tool major cutting edge inclination angle) was selected as a milling cutter. The cutting edges were made from fine-grained sintered carbide (mean grain size approx. $0.4 \mu\text{m}$) within TiAlCN anti-wear resistance coating. Experiments were conducted in free, down milling conditions, on 5-axes CNC milling workstation (DECKEL MAHO Co., model DMU 60monoBLOCK). Cutting parameters applied in the research are presented in the Table 1.

Table 1. Cutting parameters applied in the finish milling.

| a_e [mm] | a_p [mm] | z_c | a_p/p_o | f_z [mm/tooth] | n [rev/min] | v_c [m/min] | v_f [mm/min] |
|------------|------------|-------|-----------|------------------|---------------|---------------|----------------|
| 0.1 | 2 | 0.5 | 0.32 | 0.1 | 5305 | 200 | 3183 |
| 0.2 | 6.28 | 1.25 | 1 | 0.1 | 5305 | 200 | 3183 |
| 0.5 | 7 | 1.5 | 1.11 | 0.1 | 5305 | 200 | 3183 |

In the carried out research, active number of teeth z_c (related to the value of axial and radial depth of cut: a_p, a_e) was variable. This parameter significantly influences cutting force variations in function of time. Figure 3 depicts feed normal force $F_{fNe}(t)$ time courses obtained for different z_c values, calculated on the basis of model presented in [11].

In case, when active number of teeth $z_c = 0.5$, cutting forces per each tooth pulsate from 0 to the maximal value (Figure 3a). When active number of teeth $z_c = 1.25$ and a load constancy condition (quotient of axial depth of cut to axial pitch $a_p/p_o = 1$) is fulfilled, cutting force is almost constant in time. This phenomenon results from the projection of cutter with the helical cutting edges into the work piece. For the active number of teeth $z_c = 1.5$, cutting force is periodically variable from the minimal to the maximal values. In this case minimal force is different than zero, because in the whole cutting time at least 1 tooth cuts the material. Furthermore, the growth of z_c value induces the increase of maximal cutting force value, which is attributed to the growth of axial and radial depth of cut values. It is worth indicating that, when cutter's static run out is $e_r > 0$ (Figure 3b), instantaneous maximal forces per each tooth are not uniform. The alterations of these forces produce the envelope, which has a period equal to tool revolution time T . Above mentioned force variations affect cutter's displacements and thus surface texture.

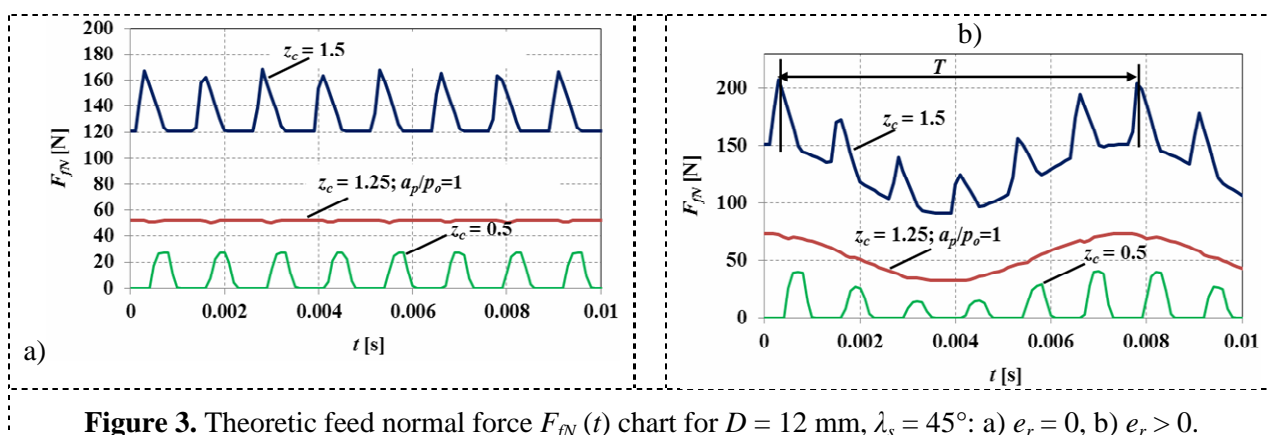


Figure 3. Theoretic feed normal force $F_{fN}(t)$ chart for $D = 12$ mm, $\lambda_s = 45^\circ$: a) $e_r = 0$, b) $e_r > 0$.

In the carried out research surface roughness topographies, cutting force components and tool displacements were measured for various z_c values. Surface roughness measurements were made using T8000 stationary surface profile meter (Hommelwerke) in the direction parallel to feed motion vector v_f . After each trial, measuring probe was moved in the direction perpendicular to

the feed motion. The measurements were repeated 50 times. As a result of these measurements 3D surface topography charts were received. The value of R_z parameter was calculated using Turbo DATAWIN software for the each measurement trial. These R_z parameter values were averaged for the 50 carried out trials. Parallel to surface roughness measurements, cutting force components were measured (in machine tool coordinates – Figure 4), in feed force F_f and feed normal force F_{fN} direction.

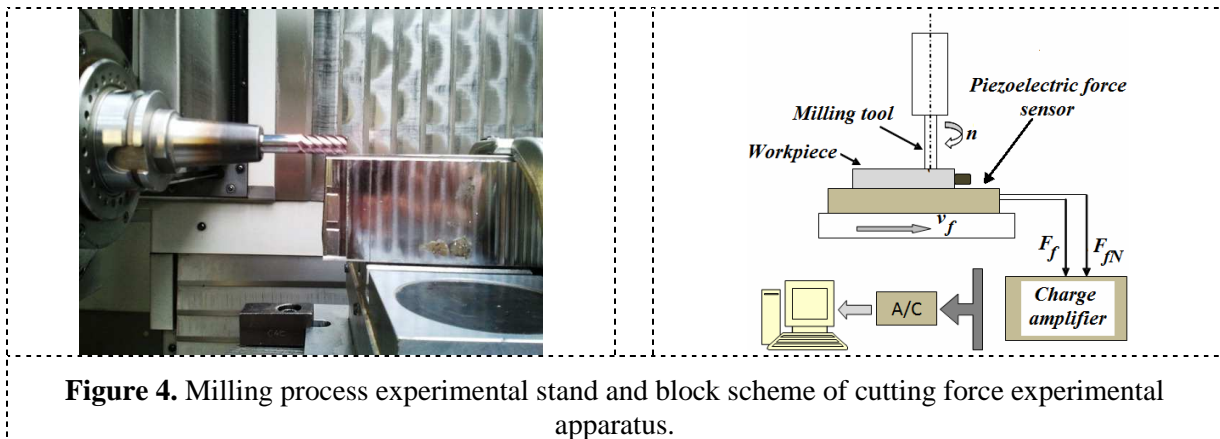


Figure 4. Milling process experimental stand and block scheme of cutting force experimental apparatus.

In order to solve differential motion equation (5), modal parameters (m , c , k) were determined using impact test, and thus the following parameters were received: $m = 0.079 \text{ Ns}^2/\text{m}$, $c = 40.8 \text{ Ns/m}$, $k = 19492469 \text{ N/m}$. Specific cutting pressures k_c , k_{cN} for the cutting force model were obtained empirically from calibration tests as: $k_c = 5440 \text{ MPa}$ and $k_{cN} = 2634 \text{ MPa}$. Differential motion equation (5) was solved in **Simulink** software equipped with **ode45** solver.

In order to measure cutter displacements during milling process, scanning laser vibrometer Polytec PSV-400 was applied. The method of measurement is described in details in [1]. The diagram depicting displacement measurement is shown in figure 5. Cutter displacement measurements were conducted in the joining part of the tool (at the distance l_m from the toolholder), because it is impossible to conduct the measurement on the working part of tool during milling. Cutter's static run out (expressed as the offset between the position of the tool rotation axis and the spindle rotation axis) was measured offline using dial indicator, and its value was $e_r = 9 \mu\text{m}$.

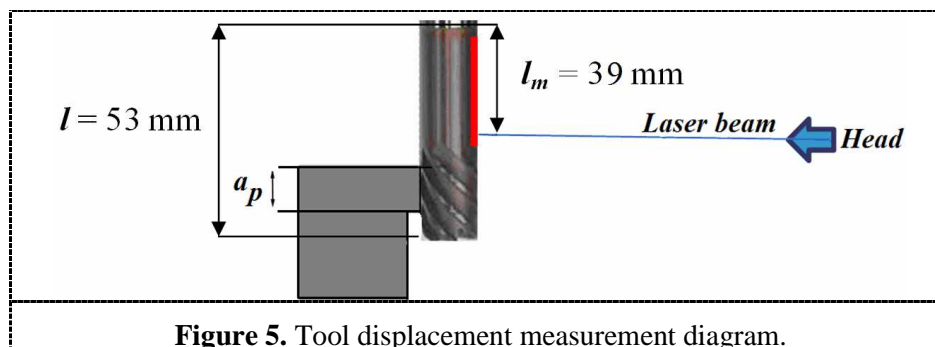


Figure 5. Tool displacement measurement diagram.

4. Research results and analysis

Figure 6 depicts measured and calculated time courses of the feed normal force component $F_{fN} = f(t)$ for the active number of teeth $z_c = 0.5$. It was found that maximal instantaneous force F_{fN} values per consecutive teeth are not uniform. Alterations of these instantaneous maximal forces produce the envelope, which has a period equal to tool revolution time. This is caused by the cutter's radial run out

phenomenon, related directly to the tool revolution period (see also Figure 3b). Similar dependencies were observed for all investigated active number of teeth. It can be also seen that instantaneous feed normal force values calculated on the basis of the developed model stay in good agreement with the measured ones.

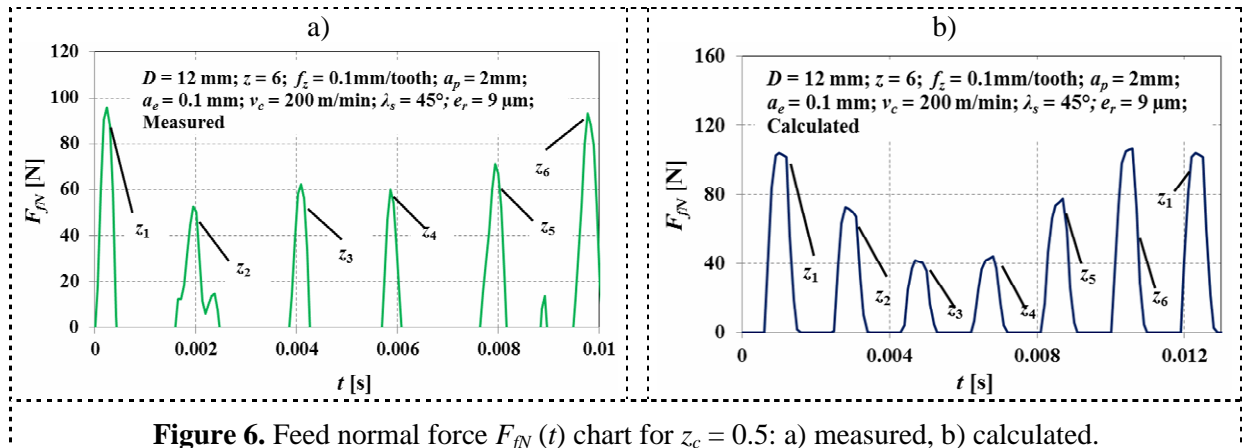
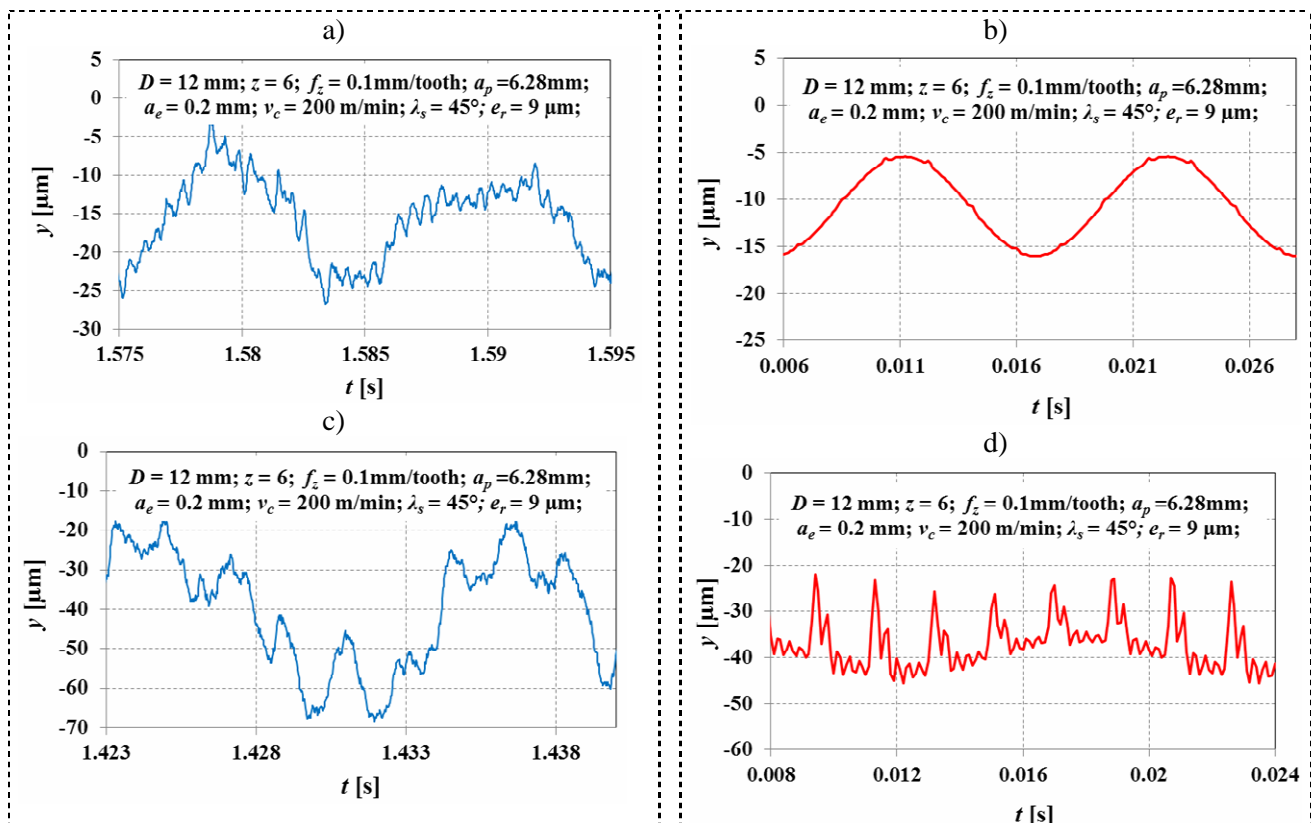


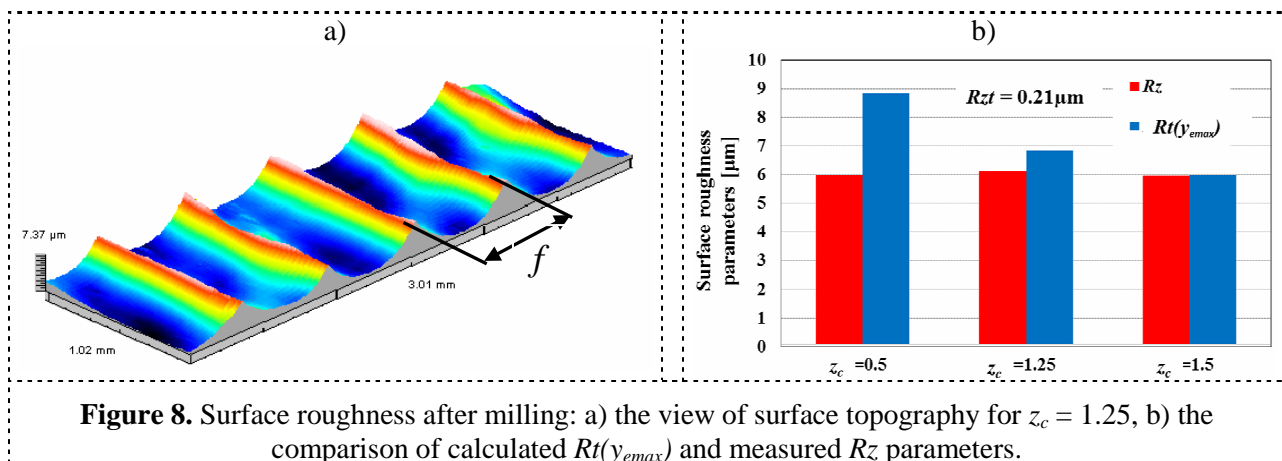
Figure 7 depicts the time course of simulated (based on equation 4), and measured cutter's displacements $y(t)$ chart for the active number of teeth $z_c = 1.25$ and $z_c = 1.5$.



In case, when active number of teeth $z_c = 1.25$ and a load constancy condition is fulfilled, the time course of calculated and measured displacements is similar to sine function, without any peaks related to the projection of teeth into the work piece. This phenomenon is attributed to the shape of the feed normal force time course (see Figure 3b), which forces cutter's displacements. Therefore, for the $z_c = 1.25$ cutter's displacements are induced mainly by the run out phenomenon. In case, when $z_c = 1.5$, cutter's displacements have different shape than those for $z_c = 1.25$. The displacement chart consists also of peaks related to the projection of teeth into the work piece, which stays in agreement with the shape of the feed normal force time course for the $z_c = 1.5$ (see figure 3b). It can be also seen that maximal instantaneous displacement values per consecutive teeth are not uniform. Alterations of these instantaneous maximal displacements produce the envelope, which results from the run out phenomenon. It is worth indicating, that displacement amplitudes have higher values for the $z_c = 1.5$. The increase in active number of teeth z_c induces higher values of cutting forces and thus higher cutter's displacement amplitudes. The cutter's displacement amplitudes have direct influence on the surface texture (e.g. surface location error – SLE).

From the figure 7 it is resulting, that simulated time course of cutter's displacements is similar to measured one, both in quantitative and qualitative aspect. Nevertheless, some discrepancies between these courses are found. They are probably resulting from the method of measurement using laser vibrometer, as well as some phenomena not included in model, i.a. the damping effect of the rigid work piece.

In all investigated cases, the condition (1) was fulfilled, and therefore surface texture was generated according to mechanism presented in Figure 1a. From the comparison of theoretical surface texture generation mechanism (Figure 1a) and measured surface topography (Figure 8a) it is resulting, that developed model including cutter's displacements stays in good agreement with the experiment. The distance between the surface irregularity peaks is equal to feed per revolution f , instead of f_z value resulting from kinematical – geometrical model. Figure 8b depicts the comparison of calculated $Rt(y_{emax})$ and measured Rz parameter values for various active number of teeth z_c . It can be found, that surface roughness parameters Rz calculated on the basis of equation (2) are similar to those measured using surface profiler, independently of active number of teeth z_c . It is worth indicating, that surface roughness value calculated on the basis of kinematical – geometrical model is barely $Rzt = 0.21 \mu\text{m}$. It proves that during finish milling this model is insufficient to the accurate surface roughness estimation. From the Figure 8b it is also resulting, that active number of teeth z_c have insignificant influence on the surface roughness parameter Rz values. The increase in active number of teeth induces the growth of cutting forces and tool's displacement (vibrations) amplitudes, which in turn affects surface location errors (SLE) and surface waviness. Nevertheless, investigations revealed, that surface roughness height Rz is affected mainly by the cutter's displacements y_e resulting from the occurrence of radial run out.



5. Conclusions

The research revealed that in finish cylindrical milling process, cutting force variations have immediate influence on surface texture generation. The increase in depths of cut, and thus active number of teeth values induces the growth of cutting forces and tool's displacement (vibrations) amplitudes, which can affect surface location errors (SLE) and surface waviness. However, surface roughness height is affected mainly by the cutter's displacements resulting from the occurrence of radial run out.

The surface roughness values R_z estimated on the basis of the developed model including cutter's displacements stay in good agreement with measured ones, what confirms the validity of applied model. The surface roughness value calculated on the basis of kinematical – geometrical model is approximately 28 times lower than the measured value, which proves that during finish milling this model is insufficient to the accurate surface roughness estimation.

The developed cutter's displacements model can be also applied to the estimation of surface location errors (SLE) and surface waviness.

6. References

- [1] Wojciechowski S, 2011 Machined surface roughness including cutter displacements in milling of hardened steel, *Metrology and Measurement Systems* Vol. **18**, **3**, 429 – 440
- [2] Urbanski J P, Koshy P, Dewes R C, Aspinwall D K, 2000 High speed machining of moulds and dies for net shape manufacture, *Materials and design* **21**, 2000, s. 395 – 402
- [3] Kawalec M, 1990 Cutting of hardened steels and cast iron with tools with defined geometry. *Dissertation* no 234, Poznan University of Technology, Poznan
- [4] Twardowski P, Wojciechowski S, Wieczorowski M, Mathia T G 2011 Selected Aspects of High Speed Milling Process Dynamics Affecting Machined Surface Roughness of Hardened Steel, *Scanning* VOL. **33**, 386–395
- [5] Wojciechowski S, Twardowski P 2011 Machined surface roughness in the aspect of milling process dynamics, *13th International Conference on Metrology and Properties of Engineering Surfaces*. 12 – 15 April 2011 Twickenham Stadium, Great Britain, p. 87 – 91
- [6] Benardos P G, Vosniakos G C 2003 Predicting surface roughness in machining: a review. *International Journal of Machine Tools & Manufacture*, **43**, p. 833-844
- [7] Schmitz T L, Couey J, Marsh E, Mauntler N, Hughes D 2007 Runout effects in milling: Surface finish, surface location error, and stability. *International Journal of Machine Tools & Manufacture* **47**, 841–851
- [8] Franco P, Estrems M, Faura F, 2004 Influence of radial and axial runouts on surface roughness in face milling with round insert cutting tools. *International Journal of Machine Tools & Manufacture* **44**, p. 1555 – 1565
- [9] Tatar K, Gren P, 2008 Measurement of milling tool vibrations during cutting using laser vibrometry. *International Journal of Machine Tools & Manufacture* **48**, p. 380 – 387
- [10] Miyaguchi T, Masuda M, Takeoka E, Iwabe H, 2001 Effect of tool stiffness upon tool wear in high spindle speed milling using small ball end mill. *Journal of the International Societies for Precision Engineering and Nanotechnology*, **25**, 145–154
- [11] Wojciechowski S, Pelic M, Twardowski P 2012 Cutter displacements as a main factor in surface texture generation during cylindrical milling of hardened steel. *ICSM 2012 International Conference on Surface Metrology, Annecy – Mont Blanc, France, March 21-23 2012*